Ann. Geophys., 24, 2823–2839, 2006
www.ann-geophys.net/24/2823/2006/

Annales Geophysicae

Model of daytime emissions of electronically-vibrationally excited products of O_3 and O_2 photolysis: application to ozone retrieval

V. A. Yankovsky and R. O. Manuilova

Institute for Physics of St. Petersburg State University, 1 Ulaynovskaya str., Petergoff, St.-Petersburg, 198504, Russia

Received: 2 February 2006 – Revised: 23 August 2006 – Accepted: 6 September 2006 – Published: 21 November 2006

Abstract. The traditional kinetics of electronically excited products of O_3 and O_2 photolysis is supplemented with the processes of the energy transfer between electronically-vibrationally excited levels $O_2(a^1\Delta_g, v)$ and $O_2(b^1\Sigma_g^+, v)$, excited atomic oxygen $O(^1D)$, and the O_2 molecules in the ground electronic state $O_2(X^3\Sigma_g^-, v)$. In contrast to the previous models of kinetics of $O_2(a^1\Delta_g)$ and O_2 $(b^1\Sigma_g^+)$, our model takes into consideration the following basic facts: first, photolysis of O_3 and O_2 and the processes of energy exchange between the metastable products of photolysis involve generation of oxygen molecules on highly excited vibrational levels in all considered electronic states – $b^1\Sigma_g^+$, $a^1\Delta_g$ and $X^3\Sigma_g^-$; second, the absorption of solar radiation not only leads to populating the electronic states on vibrational levels with vibrational quantum number v equal to 0 – $O_2(b^1\Sigma_g^+, v=0)$ (at 762 nm) and $O_2(a^1\Delta_g, v=0)$ (at 1.27 μm), but also leads to populating the excited electronic–vibrational states $O_2(b^1\Sigma_g^+, v=1)$ and $O_2(b^1\Sigma_g^+, v=2)$ (at 689 nm and 629 nm). The proposed model allows one to calculate not only the vertical profiles of the $O_2(a^1\Delta_g, v=0)$ and $O_2(b^1\Sigma_g^+, v=0)$ concentrations, but also the profiles of $[O_2(a^1\Delta_g, v\leq5)]$, $[O_2\ (b^1\Sigma_g^+, v=1, 2)]$ and $O_2(X^3\Sigma_g^-, v=1$–$35)$. In the altitude range 60–125 km, consideration of the electronic-vibrational kinetics significantly changes the calculated concentrations of the metastable oxygen molecules and reduces the discrepancy between the altitude profiles of ozone concentrations retrieved from the 762-nm and 1.27-μm emissions measured simultaneously.

Keywords. Atmospheric composition and structure (Airglow and aurora; Middle atmosphere – composition and chemistry; Thermosphere – composition and chemistry)

Correspondence to: V. A. Yankovsky
(valentine.yankovsky@paloma.spbu.ru)

1 Introduction

Measurements of radiation of electronically excited molecular oxygen in the Atmospheric band $O_2(b^1\Sigma_g^+, v=0\rightarrow X^3\Sigma_g^-, v=0)$ at 762 nm and in the Infrared Atmospheric band $O_2(a^1\Delta_g, v=0\rightarrow X^3\Sigma_g^-, v=0)$ at 1.27 μm are used for retrieving the altitude profile of ozone concentration (e.g. Thomas et al., 1984; Mlynczak et al., 2001). Interpretation of the measurements of emission at 1.27 μm is a well known method of determination of the altitude profile of ozone concentration, and emission at 762 nm was also suggested for this goal in Sica and Lowe (1993a, b). Both methods were realized in Mlynczak et al. (2001). Nowadays, interest in the models of these emissions grows due to the measurements in which both emissions were measured simultaneously in a rocket (Mlynczak et al., 2001) and especially in a satellite experiment (Murtagh et al., 2002).

Metastable molecules and atoms of oxygen are formed in the processes of photodissociation of ozone and oxygen molecules at absorption of ultra-violet radiation of the Sun. These excited products of O_3 and O_2 photolysis play an important role in the electronic-vibrational kinetics of O_2 molecules and in the heating of the middle atmosphere. The first commonly accepted model of electronic kinetics of these products was developed by Thomas (1984) and Harris and Adams (1983) and was significantly improved by Mlynczak et al. (1993). At present, the model of the electronic kinetics of the products of O_3 and O_2 photolysis, developed by Mlynczak et al. (1993), is used. Let's describe briefly the processes which were taken into account in this model. Photolysis of oxygen in the Schumann-Runge continuum and in the Lyman alpha (Lyman-α) line leads to the formation of the atomic oxygen in the first excited electronic state $O(^1D)$. Photolysis of ozone in the Hartley band also leads to the formation of the $O(^1D)$ atom and of the oxygen molecule in the first excited electronic singlet state $O_2(a^1\Delta_g)$. The processes of energy transfer from the $O(^1D)$ state to the second

Published by Copernicus GmbH on behalf of the European Geosciences Union.

excited electronic state of the O_2 molecule $O_2(b^1\Sigma_g^+)$ and, further, to the first electronic excited state $O_2(a^1\Delta_g)$, play an important role in populating these two electronic states. All these excited states of atomic and molecular oxygen $O(^1D)$, $O_2(b^1\Sigma_g^+)$, and $O_2(a^1\Delta_g)$ radiate. The corresponding O_2 emissions take place in the Atmospheric band:

$$O_2(b^1\Sigma_g^+, v{=}0) \rightarrow O_2(X^3\Sigma_g^-, v{=}0) + h\nu(\lambda{=}762\,\text{nm}) \quad (1)$$

and in the Infrared (IR) Atmospheric band:

$$O_2(a^1\Delta_g, v{=}0) \rightarrow O_2(X^3\Sigma_g^-, v{=}0) + h\nu(\lambda{=}1.27\,\mu\text{m}), \quad (2)$$

where v is vibrational quantum number. These emissions are observed using a modern experimental technique. With the use of the kinetic scheme, suggested in Mlynczak et al. (1993), vertical profiles of the ozone abundance are retrieved from the observations of vertical profiles of these emissions (Mlynczak et al., 2001). At photolysis of ozone in the Hartley band, $O_2(a^1\Delta_g)$ is formed with the quantum yield about 90%. It seems evident that the Infrared Atmospheric band of O_2 at 1.27 μm (2), that is formed by transition from $O_2(a^1\Delta_g)$, is preferable for retrieving the profiles of ozone abundance. This point of view is traditional up to present. However, simultaneously with the production of $O_2(a^1\Delta_g)$, the $O(^1D)$ atom is formed with the same quantum yield. Therefore, the ozone abundance retrieval could also be carried out using the emission from the state $O_2(b^1\Sigma_g^+)$ at 762 nm (Eq. 1). In the framework of the kinetic model suggested in Mlynczak et al. (1993), it is impossible to determine which method of retrieval is more accurate.

Beginning with the publications of the studies of Sparks et al. (1980), Valentini et al. (1987), Thelen et al. (1995), it has been known that the products of O_3 photolysis must also be vibrationally excited. Besides that, energy transfer from $O(^1D)$ to O_2 leads to the formation of electronically-vibrationally excited molecules $O_2(b^1\Sigma_g^+, v)$ (Streit et al., 1976; Lee and Slanger, 1978). Mlynczak et al. (1993) supposed that vibrational kinetics can be neglected, which is possible only if the processes of vibrational-vibrational (V-V) and vibrational-translational (V-T) energy transfer between vibrational sublevels of electronic states are much faster than collisional deactivation of electronically excited states. However, the present laboratory and theoretical data on the kinetics of the excited products of ozone and oxygen photolysis (Hwang et al., 1999; Slanger and Copeland, 2003; Dylewski et al., 2001; Kalogerakis et al., 2002; Pejakovic et al., 2005) have given new information about the processes of energy exchange between electronic-vibrational levels, which are fast enough to compete with the processes of V-V and V-T energy exchange. These works made it necessary to create a model of electronic-vibrational kinetics of the excited products of O_3 and O_2 photolysis because the fast processes of energy exchange between electronically-vibrationally excited levels could not be considered in the framework of only electronic kinetics. It should also be noted, that transitions $O_2(b^1\Sigma_g^+, v{\rightarrow}X^3\Sigma_g^-, v'')$ have also been observed in atmospheric experiments. Skinner and Hays (1985), analyzing the brightness of the Atmospheric band of O_2 in the daytime thermosphere measured by the Dynamic Explorer 2 in the altitude interval 60–300 km, took into account the contributions of transitions $O_2(b^1\Sigma_g^+, v{\rightarrow}X^3\Sigma_g^-, v'')$ for bands (0-0), (1-1), (2-2). We will show in this study that the traditional kinetics of electronically excited products of O_3 and O_2 photolysis should be supplemented with the processes of energy transfer between electronically-vibrationally excited levels $O_2(a^1\Delta_g, v)$ and $O_2(b^1\Sigma_g^+, v)$, excited atomic oxygen $O(^1D)$ and the O_2 molecules in the ground electronic state $O_2(X^3\Sigma_g^-, v)$. In contrast to the previous models of kinetics of $O_2(a^1\Delta_g)$ and O_2 $(b^1\Sigma_g^+)$, our model takes into consideration the following basic facts: first, photolysis of O_3 and O_2 and the processes of energy exchange between the metastable products of photolysis involve generation of oxygen molecules on highly excited vibrational levels in all considered electronic states – $b^1\Sigma_g^+$, $a^1\Delta_g$ and $X^3\Sigma_g^-$; second, the absorption of solar radiation not only leads to populating the electronic states on vibrational levels with vibrational quantum number v equal to 0 – $O_2(b^1\Sigma_g^+, v{=}0)$ (at 762 nm) and $O_2(a^1\Delta_g, v{=}0)$ (at 1.27 μm), but also leads to populating the excited electronic–vibrational states $O_2(b^1\Sigma_g^+, v{=}1)$ and $O_2(b^1\Sigma_g^+, v{=}2)$ (at the 689 nm and 629 nm). In the framework of this study we will compare the models of pure electronic and electronic-vibrational kinetics and show the difference between the two models for the direct problem of calculations of the volume emission rates of the 762-nm and 1.27-μm bands and for the inverse problem of ozone retrieval from both emissions. As it will be shown below, considering the electronic-vibrational kinetics significantly changes the calculated concentrations of the metastable oxygen molecules above 60 km and reduces the discrepancy between the altitude profiles of ozone concentrations retrieved from the 762-nm and 1.27-μm emissions measured simultaneously.

2 Kinetics of electronically-vibrationally excited products of O_3 and O_2 photodissociation in the middle atmosphere

In Fig. 1, the scheme of electronic-vibrational kinetics of the products of O_3 and O_2 photolysis is presented. The excited electronic states are shown by bold lines, and the vibrational levels of these electronic states are shown by thin lines. The vibrational number is denoted by the letter v. The circles with italic letters in Fig. 1 denote all types of processes that were taken into account. References to the values of the rates of photodissociation of O_2 and O_3 and of photoexcitation of O_2 used in this study are presented in Table 1, and references to the values of the rate constants of the considered processes are presented in Tables 2–5. Let's describe the processes under consideration.

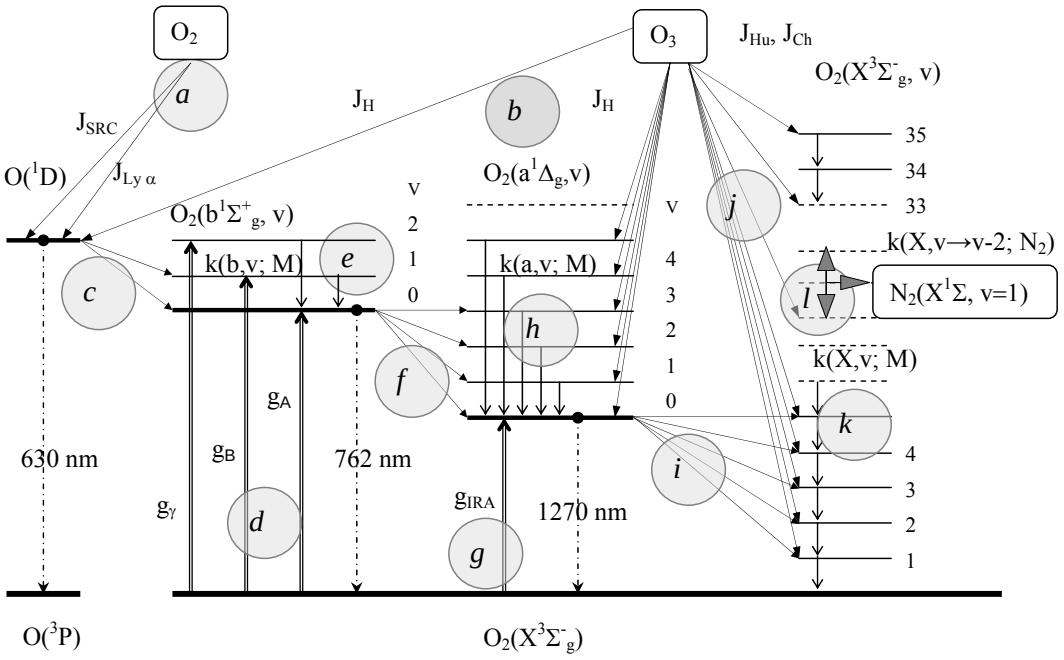

Fig. 1. The scheme of electronic-vibrational kinetics of the products of O_3 and O_2 photolysis in the middle atmosphere.

Table 1. Processes of O_2 and O_3 photodissociation and photoexcitation. Short notations for electronically excited states of oxygen molecule in Tables 1–5: $O_2(b^1\Sigma_g^+, v)=O_2(b, v)$, $O_2(a^1\Delta_g, v)=O_2(a, v)$, $O_2(X^3\Sigma_g^-, v)=O_2(X, v)$. J – rate of photodissociation and photoexcitation at the top of the atmosphere, F – quantum yield of the products.

Reaction	J (s^{-1})	F	Ref.
$O_2+h\nu$(SRC)$\rightarrow O(^3P)+O(^1D)$	2.60×10^{-6}	1.0	Rodrigo et al. (1986), DeMore et al. (1997)
$O_2+h\nu$(Lyman-α)$\rightarrow O(^3P)+O(^1D)$	3.40×10^{-9}	0.48–0.58	Rodrigo et al. (1986), Reddmann and Uhl (2003)
$O_3+h\nu\rightarrow O_2$(X, v=0–35)$+O(^3P)$	8.00×10^{-3}	0.10*	Svanberg et al. (1995)
$O_3+h\nu\rightarrow O_2$(a, 5)$+O(^1D)$		0.045*	Michelson et al. (1994),
$O_3+h\nu\rightarrow O_2$(a, 4)$+O(^1D)$		0.072*	Sparks et al. (1980),
$O_3+h\nu\rightarrow O_2$(a, 3)$+O(^1D)$		0.072*	Thelen et al. (1995),
$O_3+h\nu\rightarrow O_2$(a, 2)$+O(^1D)$		0.135*	Valentini et al. (1987),
$O_3+h\nu\rightarrow O_2$(a, 1)$+O(^1D)$		0.135*	Ball et al. (1995),
$O_3+h\nu\rightarrow O_2$(a, 0)$+O(^1D)$		0.441*	Klais et al. (1980), DeMore et al. (1997), Dylewski et al. (2001)
$O_2+h\nu$(762 nm band)$\rightarrow O_2$(b, 0)	5.35×10^{-9}		Bucholtz et al. (1986), Mlynczak et al. (1996)
$O_2+h\nu$ (689 nm band)$\rightarrow O_2$(b, 1)	2.94×10^{-10}		
$O_2+h\nu$ (629 nm band)$\rightarrow O_2$(b, 2)	7.94×10^{-12}		
$O_2+h\nu$ (1.27 μm)$\rightarrow O_2$(a, 0)	1.54×10^{-10}		

* – Presented values are quantum yields for λ=254 nm, however, all calculations of the rate of O_3 photodissociation in the Hartley band are carried out for the values of quantum yields depending on wave length (Yankovsky and Kuleshova, 2006).

Table 2. Processes of $O(^1D)$ deactivation. A – Einstein coefficient, K – rate constant of reaction, other symbols as in Table 1.

Reaction	A (s^{-1}), K ($cm^3\,s^{-1}$)	F	Ref.
$O(^1D)\rightarrow O+h\nu$ (630 nm)	9.0×10^{-3}		DeMore et al. (1997)
$O(^1D)+O\rightarrow 2O$	4.0×10^{-12}		Yee et al. (1990)
$O(^1D)+O_2\rightarrow O_2(b,1)+O$	$3.2\times10^{-11}\,e^{67/T}$	0.40	Streit et al. (1976), Lee and Slanger (1978), Green et al. (2000)
$O(^1D)+O_2\rightarrow O_2(b,0)+O$		0.55	
$O(^1D)+O_2\rightarrow O_2(a,0\text{ or }X,0)+O$		$\leq$0.05	
$O(^1D)+O_3\rightarrow 2O_2$	2.4×10^{-10}		Atkinson et al. (1997)
$O(^1D)+N_2\rightarrow O+N_2$	$2.0\times10^{-11}\,e^{107/T}$	0.67	DeMore et al. (1997), Tully (1974)
$O(^1D)+N_2\rightarrow O+N_2(v\leq7)$		0.33	

a – photolysis of O_2 in the Schumann-Runge continuum (SRC) in the 120–174-nm region and in the Lyman-α line (Table 1):

$$O_2 + h\nu\ (\text{SRC, Lyman}-\alpha) \rightarrow O(^1D) + O(^3P); \quad (3)$$

these processes are the main sources of $O(^1D)$ atoms above 80 km (e.g. Rodrigo et al., 1986);

b – photolysis of O_3 in the singlet channel (the Hartley band at 200–310 nm) (Table 1):

$$O_3+h\nu\ (\text{the Hartley band}) \rightarrow O_2(a^1\Delta_g, v{=}0{-}5)+O(^1D); \quad (4)$$

c – EE′ transfer of electronic excitation energy from the $O(^1D)$ atom to the oxygen molecule. The process of energy transfer from $O(^1D)$ excites not only vibrational level 0, but also vibrational level 1 of the electronic state $O_2(b^1\Sigma_g^+)$ (Table 2):

$$O(^1D)+O_2(X^3\Sigma_g^-,\ \text{v=0}) \rightarrow O_2(b^1\Sigma_g^+, v\leq 1)+O(^3P); \quad (5)$$

d – excitation of all three considered vibrational levels of the electronic state $O_2(b^1\Sigma_g^+)$ due to direct absorption of solar radiation. The rates of absorption at 762, 689 and 629 nm were taken from Bucholtz et al. (1986); Mlynczak and Marshall (1996) (Table 1):

$$O_2 + h\nu\ (762;\ 689;\ 629\,\text{nm}) \rightarrow O_2(b^1\Sigma_g^+, v{=}0,\ 1,\ 2), \quad (6)$$

respectively;

e – quenching of vibrational excitation of $O_2(b^1\Sigma_g^+,\ v\geq1)$ due to intramolecular near resonance electronic-electronic (EE) exchange (Table 3):

$$O_2(b^1\Sigma_g^+, v\leq 2) + O_2(X^3\Sigma_g^-,\ v{=}0) \rightarrow O_2(X^3\Sigma_g^-,\ v\leq 2) + O_2(b^1\Sigma_g^+, v{=}0); \quad (7)$$

a specific feature of this type of reaction is that the electronic level changes in the initially excited oxygen molecule, while the vibrational quantum number v remains unchanged, and electronic excitation transfers to the collisional partner. Such reactions are from 2 to 3 orders of magnitude faster than the reactions of intermolecular energy transfer between electronic levels (reactions of the type ***f*** in Fig. 1);

f – formation of $O_2(a^1\Delta_g,\ v{=}0{-}3)$ at collisional quenching of $O_2(b^1\Sigma_g^+,\ v{=}0)$ by the electronic-vibrational (EV) type of the energy exchange (Table 2):

$$O_2(b^1\Sigma_g^+,\ v{=}0) + M(=O_2,\ N_2,\ O(^3P), O_3, CO_2) \rightarrow O_2(a^1\Delta_g, v\leq 3) + M; \quad (8)$$

g – the process of excitation of $O_2(a^1\Delta_g,\ v{=}0)$ due to direct absorption of solar radiation (Table 1):

$$O_2 + h\nu(1.27\,\mu\text{m}) \rightarrow O_2(a^1\Delta_g, v{=}0); \quad (9)$$

h – the process of EE quenching of $O_2(a^1\Delta_g,\ v)$, similar to the channel ***e*** (Table 4):

$$O_2(a^1\Delta_g, v) + O_2(X^3\Sigma_g^-,\ v{=}0) \rightarrow O_2(X^3\Sigma_g^-, v) + O_2(a^1\Delta_g,\ v{=}0); \quad (10)$$

i – quenching of O_2 $(a^1\Delta_g,\ v{=}0)$ of the type similar to EV-exchange (Table 4):

$$O_2(a^1\Delta_g,\ v{=}0) + O_2(X^3\Sigma_g^-,\ v{=}0) \rightarrow O_2(X^3\Sigma_g^-, v\leq 5) + O_2(X^3\Sigma_g^-, v''{=}5{-}v); \quad (11)$$

j – excitation of the vibrational levels of the ground electronic state $O_2(X^3\Sigma_g^-,\ v)$ at ozone photolysis in the triplet channel (the Hartley, Huggins, and Chappius bands in the region from 200 to 600 nm); these levels are excited up to v=35 (Table 1):

$$O_3 + h\nu \rightarrow O_2(X^3\Sigma_g^-, v\leq 35) + O(^3P); \quad (12)$$

Table 3. Processes of deactivation of $O_2(b^1\Sigma_g^+, v)$. Symbols as in Tables 1 and 2.

Reaction	A (s^{-1}), K ($cm^3\,s^{-1}$)	F	Ref.
$O_2(b, 2) \rightarrow O_2(X, 2)+h\nu$ (780 nm)	5.4×10^{-2}		Yankovsky (1991)
$O_2(b, 2)+O \rightarrow O_2(b, 1)+O$	1.1×10^{-11}		
$O_2(b, 2)+O_2 \rightarrow O_2(X, 2)+O_2(b, 0)$	$1.2\times10^{-11}\,e^{-596/T}$ 3.15×10^{-12}		Kalogerakis et al. (2002), Yankovsky (1991)
$O_2(b, 2)+N_2 \rightarrow O_2(b, 1)+N_2$	$<2\times10^{-14}$		Hwang et al. (1999)
$O_2(b, 2)+O_3 \rightarrow 2O_2+O$	2.9×10^{-10}		Yankovsky (1991)
$O_2(b, 1) \rightarrow O_2(X, 1)+h\nu$ (771 nm)	7.0×10^{-2}		Krupenie (1972)
$O_2(b, 1)+O \rightarrow O_2(b, 0)+O$	4.5×10^{-12}		Pejakovic et al. (2005)
$O_2(b, 1)+O_2 \rightarrow O_2(X, 1)+O_2(b, 0)$	$4.2\times10^{-11}\,e^{-312/T}$		Kalogerakis et al. (2002)
$O_2(b, 1)+N_2 \rightarrow O_2(b, 0)+N_2$	$<5\times10^{-13}$		Hwang et al. (1999)
$O_2(b, 1)+O_3 \rightarrow 2O_2+O$	$<3\times10^{-10}$		Yankovsky (1991)
$O_2(b, 0) \rightarrow O_2(X, 0)+h\nu$ (762 nm)	7.58×10^{-2}		Mlynczak et al. (1993)
$O_2(b, 0)+O \rightarrow O_2(a, 0)+O$	8.0×10^{-14}	0.75	Atkinson et al. (1997), Hady-Ziane et al. (1992)
$O_2(b, 0)+O \rightarrow O_2(X, 0)+O$		0.25	
$O_2(b, 0)+O_2 \rightarrow O_2(a, 0)+O_2(X, 3)$		0.230	
$O_2(b, 0)+O_2 \rightarrow O_2(a, 1)+O_2(X, 2)$	3.9×10^{-17}	0.525	Klingshirn and Maier (1985)
$O_2(b, 0)+O_2 \rightarrow O_2(a, 2)+O_2(X, 1)$		0.226	
$O_2(b, 0)+O_2 \rightarrow O_2(a, 3)+O_2(X, 0)$		0.019	
$O_2(b, 0)+N_2 \rightarrow$ products	2.1×10^{-15}		Atkinson et al. (1997), see text
$O_2(b, 0)+CO_2 \rightarrow O_2(a, 0)+CO_2$	4.2×10^{-13}		Atkinson et al. (1997)
$O_2(b, 0)+O_3 \rightarrow O_2(a, 0)+O_3$	2.2×10^{-11}	0.3	Amimoto et al. (1980), Atkinson et al. (1997)

k – the processes of vibrational-vibrational (V-V) and vibrational-translational (V-T) deexcitation of vibrational levels $O_2(X^3\Sigma_g^-, v)$ for v=1–35 (Table 5):

$$O_2(X^3\Sigma_g^-, v \le 35) + O_2(X^3\Sigma_g^-, v{=}0) \rightarrow O_2(X^3\Sigma_g^-, v{-}1) + O_2(X^3\Sigma_g^-, v{=}1), \quad (13)$$

$$O_2(X^3\Sigma_g^-, v \le 35) + M(=O_2,\ N_2,\ O(^3P),\ O_3) \rightarrow O_2(X^3\Sigma_g^-, v{-}1) + M; \quad (14)$$

l – the process of VV two-quantum transition in collisions of $O_2(X^3\Sigma_g, v)$ with N_2 for v=12–26 (Table 5):

$$O_2(X^3\Sigma_g^-, 12 \le v \le 26) + N_2(X^1\Sigma, v{=}0) \rightarrow O_2(X^3\Sigma_g^-, v{-}2) + N_2(X^1\Sigma, v{=}1). \quad (15)$$

The vibrational levels of the ground electronic state are populated by the processes of electronic-vibrational (EV) energy exchange with the state $O_2(a^1\Delta_g, v{=}0)$ (Eq. 11). As it was noted above, at ozone photolysis in the Hartley, Huggins and Chappius bands, the vibrational levels of the ground electronic level $O_2(X^3\Sigma_g^-, v)$ are excited up to the value of v=35 (Eq. 12). Other processes which populate vibrational levels are the processes of EE exchange with the corresponding levels of the electronic states $O_2(b^1\Sigma_g^+, v)$ for v=0–2 (Eq. 6) and $O_2(a^1\Delta_g, v)$ for v=1–5 (Eq. 10).

In Table 1 the rates of photodissociation of O_2 and O_3 and of photoexcitation of $O_2(b^1\Sigma_g^+, v)$ and $O_2(a^1\Delta_g, v{=}0)$ used in this study are presented. The quantum yield of $O(^1D)$ formation in the O_2 photolysis in the Schumann-Runge continuum is equal to 1 (DeMore et al., 1997). For O_3 photolysis in

Table 4. Processes of deactivation of $O_2(a^1\Delta_g, v)$. Symbols as in Tables 1 and 2.

Reaction	A (s^{-1}), K ($cm^3\,s^{-1}$)	F	Ref.
$O_2(a, 0)\rightarrow O_2(X, 0)+h\nu$ (1.27 μm)	2.58×10^{-4}		Krupenie (1972)
$O_2(a, v\geq1)\rightarrow O_2+h\nu$	2.58×10^{-4}		as $O_2(a, 0)\rightarrow O_2+h\nu$
$O_2(a, v\geq3)+O_2\rightarrow O_2(X, v)+O_2(a, 0)$	3.6×10^{-11}		see text
$O_2(a, 2)+O_2\rightarrow O_2(X, 2)+O_2(a, 0)$	3.6×10^{-11}		Slanger and Copeland (2003)
$O_2(a, v\geq1)+O\rightarrow O_2+O$	$10^{-13}-10^{-16}$		see text
$O_2(a, 1)+O_2\rightarrow O_2(X, 1)+O_2(a, 0)$	5.6×10^{-11}		Slanger and Copeland (2003)
$O_2(a, 1)+O_3\rightarrow 2\times O_2+O$	4.7×10^{-12}		Klais et al. (1980)
$O_2(a, 0)+O\rightarrow O_2+O$	6.5×10^{-17}		Lopez-Gonzalez et al. (1992)
$O_2(a, 0)+O_2\rightarrow O_2(X, 5)+O_2(X, 0)$	$3.6\times10^{-18}\,e^{-220/T}$	0.014	Atkinson et al. (1997), Wild et al. (1984)
$O_2(a, 0)+O_2\rightarrow O_2(X, 4)+O_2(X, 1)$		0.214	
$O_2(a, 0)+O_2\rightarrow O_2(X, 3)+O_2(X, 2)$		0.772	
$O_2(a, 0)+O_3\rightarrow O_2+O_3$	$5.2\times10^{-11}\,e^{-2840/T}$		Atkinson et al. (1997)
$O_2(a, 0)+N_2\rightarrow O_2+N_2$	1.0×10^{-20}		DeMore et al. (1997)

Table 5. Processes of energy transfer and deactivation of $O_2(X^3\Sigma_g^-, v)$. Symbols as in Tables 1 and 2.

Reaction	K ($cm^3\,s^{-1}$)	F	Ref.
$O_3+O\rightarrow O_2(X, v=0–30)+O_2$	$5.6\times10^{-12}\,e^{-1959/T}$	F(v)	Balakrishnan and Billing (1996)
$O_2(X, v\geq5)+O\rightarrow O_2+O$	$K_{VT}=5\times10^{-11}\times(T/300)^{0.5}$		Breig (1969), Webster and Bair (1972)
$O_2(X, v=2–4)+O\rightarrow O_2+O$	$K_{VT}(v)^*=1.1\times10^{-12}\times(T/300)\,e^{1.0\cdot v}$		
$O_2(X, v=1)+O\rightarrow O_2+O$	$K_{VT}=3\times10^{-12}$		Slanger and Copeland (2003)
$O_2(X, v)+O_2\rightarrow O_2(X, v–1)+O_2(X, v=1)$	$K_{VV}(v=2)=2.0\times10^{-13}$ $K_{VV}(v=3)=2.6\times10^{-13}$		Kalogerakis et al. (2005)
$O_2(X, v=4–20)+O_2\rightarrow O_2(X, v\text{-}1)+O_2(X, 1)$	$K_{VV}(v)^*=1.3\times10^{-12}\,e^{-0.31\cdot v}$		Slanger (1997), Coletti and Billing (2002)
$O_2(X, v>20)+O_2\rightarrow O_2(X, v–1)+O_2$	$K_{VT}(v)^*=6\times10^{-17}\times(T/300)\,e^{0,2\cdot v}$		
$O_2(X, v=12–17)+N_2\rightarrow O_2(X, v–2)+N_2(X, v=1)$	$K_{VV'}(v)^*=3.6\times10^{-19}\,e^{0,66\cdot v}$		Slanger (1997)
$O_2(X, v=18–26)+N_2\rightarrow O_2(X, v–2)+N_2(X, v=1)$	$K_{VV'}(v)^*=4.5\times10^{-13}\,e^{-0,173\cdot v}$		
$O_2(X, v=1)+O_2\rightarrow 2O_2$	$K_{VT}=4.2\times10^{-19}\times(T/300)^{0,5}$		Lopez-Puertas et al. (1995)
$O_2(X, v=1)+N_2\rightarrow O_2+N_2(X, v=1)$	$K_{VV'}(v)=4.2\times10^{-19}\times(T/300)^{0.5}$		

$K_{VV}(v)^*$, $K_{VT}(v)^*$ – approximations of the experimental data made by the authors and used in this study.

the Hartley bands, the spectral dependence of quantum yield of $O(^1D)$ and, correspondingly, of $O_2(a^1\Delta_g)$, is known in detail (Michelsen et al., 1994). For $O_2(a^1\Delta_g, v)$, the quantum yields significantly depend on wave length (Sparks et al., 1980; Valentini et al., 1987; Thelen et al., 1995). The quantum yields of $O_2(a^1\Delta_g, v)$ were measured for 6 wavelengths for v=0–7 from 235 to 285 nm (Dylewski et al., 2001). These data show that the part of the electronically-vibrationally excited molecules produced at O_3 photolysis changes from 30% at 285 nm to 70% at 235 nm. At the Hartley band maximum in the region of 254 nm this part is about 60%. This is why for $O_2(a^1\Delta_g, v)$ the quantum yields should be known at all wavelengths. With the purpose of presenting the quantum yield as a function of wavelength, we constructed interpolated formulas for quantum yield dependence on the wave numbers in the whole interval of the Hartley band 200–320 nm, for all vibrational quantum numbers from 0 to 5 (Yankovsky and Kuleshova, 2006), using all published experimental data. In particular, it enables us to calculate the total production rate of $O_2(a^1\Delta_g, v)$ in O_3 photodissociation in the Hartley band by integration of these functions, the rates of photodissociation and the cross sections of solar radiation absorption over the wavelength. The vibrational levels with v equal to 6 and 7 are excited by radiation, with the wavelength shorter than 240 nm, for which the cross section of O_2 absorption is small and the processes of excitation of the levels with v=6, 7 can be neglected.

The triplet channel of O_3 photodissociation in the Hartley band gives the formation of $O_2(X^3\Sigma_g^-, v=0–35)$. The quantum yields of $O_2(X^3\Sigma_g^-, v)$ also depend significantly on the wavelength. We used the calculations of the quantum yields of $O_2(X^3\Sigma_g^-, v)$ in the Hartley band from Svanberg et al. (1995). At O_3 photodissociation in the Chappius and Huggins bands the levels $O_2(X^3\Sigma_g^-, v)$ are formed at v=0–15. The cross section of the absorption of solar radiation in the Chappius and Huggins bands is small, so the O_3 photodissociation in the Chappius and Huggins bands does not influence the production of $O_2(X^3\Sigma_g^-, v)$ significantly.

In Table 2, the Einstein coefficient for emission of $O(^1D)$ at 630 nm and the rate constants of $O(^1D)$ deexcitation at collisional processes, as well as the quantum yields of electronically-vibrationally excited products of these processes, are presented. In Green et al. (2000) the total quantum yield of $O_2(b^1\Sigma_g^+, v\geq0)$ in the reaction $O(^1D)+O_2\rightarrow O_2(b^1\Sigma_g^+, v\geq0)+O$ was estimated to be equal to 0.95. In correspondence with the value of the total quantum yield we calculated the quantum yields of $O_2(b^1\Sigma_g^+, v=1)$ and $O_2(b^1\Sigma_g^+, v=0)$, based on the results of Lee and Slanger (1978).

In Table 3, the Einstein coefficients for emissions of $O_2(b^1\Sigma_g^+, v)$ at 780, 771, and 762 nm and the rate constants of deexcitation of $O_2(b^1\Sigma_g^+, v)$ at collisional processes, as well as the quantum yields of $O_2(a^1\Delta_g, v)$ and $O_2(X^3\Sigma_g^-, v)$ for v from 0 to 3 formed in these processes, are presented. The rate constant of the reaction $O_2(b^1\Sigma_g^+, v=2)+O_2(X^3\Sigma_g^-, v=0)\rightarrow O_2(X^3\Sigma_g^-, v=2)+O_2(b^1\Sigma_g^+, v=0)$ was measured in the experiment of Kalogerakis et al. (2002) in the temperature range 110–298 K and in the experiment of Yankovsky (1991) in the range 340–445 K. Both sets of the data correspond to each other. In our calculations we used our approximation of the data of Kalogerakis et al. (2002).

For processes of deexcitation of the states $O_2(b^1\Sigma_g^+, v=1, 2)$ by N_2 only the upper limit of the values of the rate constants are known. Our estimations show that these reactions don't influence the populations of the states $O_2(b^1\Sigma_g^+, v=1, 2)$. In Tables 3 and 4 the processes of quenching the states $O_2(b^1\Sigma_g^+, v)$ and $O_2(a^1\Delta_g, v)$ at collisions with O_3 are shown in connection with high values of the rate constants of these processes. However, in the mesosphere the role of such processes is insignificant because of low abundance of ozone.

We should discuss the influence of the possible values of quantum yields of the products of the reaction of quenching of $O_2(b^1\Sigma_g^+, v=0)$ by N_2. In the model of Mlynczak et al. (1993) it is supposed that the quantum yield F(a, 0) of the process

$$O_2(b^1\Sigma_g^+, v=0) + N_2 \rightarrow O_2(a^1\Delta_g, v=0) + N_2(X, v=2) + 607.1\,cm^{-1} \quad (16)$$

is equal to 1. However, the rate constant of the reaction of quenching of $O_2(b^1\Sigma_g^+, v=0)$ by N_2 is almost 100 times greater than the rate constant of the reaction of quenching $O_2(b^1\Sigma_g^+, v=0)$ by O_2. In the framework of electronic-vibrational kinetics, possible pathways of the process of quenching of $O_2(b^1\Sigma_g^+, v=0)$ by N_2 should be considered. The relatively high value of the rate constant for quenching by N_2, led Braithwaite et al. (1976) to the suggestion that the following quasi-resonance process might exist:

$$O_2(b^1\Sigma_g^+, v=0) + N_2 \rightarrow O_2(a^1\Delta_g, v=2) + N_2(X, v=1) - 31.9\,cm^{-1}. \quad (17)$$

However, another quasi-resonance process is also possible:

$$O_2(b^1\Sigma_g^+, v=0) + N_2 \rightarrow O_2(X^3\Sigma_g^-, v=9) + N_2(X, v=0) - 52.8\,cm^{-1}. \quad (18)$$

There is no information about possible values of the quantum yields of the products of this reaction; however, the ratio between the two pathways of the reaction influence distinctly the ozone concentration retrieval at the region of the second ozone maximum. This is why we consider the suggestion that both quasi-resonance processes (Eqs. 17, 18) exist and are assumed to have the same values of the quantum yields $O_2(a^1\Delta_g, v=2)$, F(a, 2), and $O_2(X^3\Sigma_g^-, v=9)$, F(X, 9). For our calculations we used F(a, 2) and F(X, 9) equal to 0.5.

In Table 4, the Einstein coefficients for emission of $O_2(a^1\Delta_g, v)$ and the rate constants of deexcitation of $O_2(a^1\Delta_g, v)$ at collisional processes are presented. The Einstein coefficient for emission of $O_2(a^1\Delta_g, v=0)$ at 1.27 μm

was taken from Krupenie (1972). For the Einstein coefficients for emissions of $O_2(a^1\Delta_g, v=1–5)$ the same value was used, because the experimental data are absent. However, radiative deexcitation of $O_2(a^1\Delta_g, v\geq1)$ can be neglected in the calculations of O_2 $(a^1\Delta_g, v)$ concentration, due to the fact that the rate of radiative deexcitation is much smaller than the rates of deexcitation at collisions with O_2 (Slanger and Copeland, 2003).

The rate constants of deexcitation of $O_2(a^1\Delta_g, v\geq3)$ in collisions with O_2 have not been measured and for these processes we used the value of the rate constant of the process $O_2(a^1\Delta_g, v=2)+O_2$ that was measured by Slanger and Copeland (2003). For the processes of collisions of $O_2(a^1\Delta_g, v\geq1)$ with atomic oxygen the rate constants have not been measured either. So we varied the values of the rate constants of these processes from 10^{-13} to $10^{-16}\,cm^3\,s^{-1}$. Even for such a broad range of the values of the rate constants these processes do not affect the results of the calculations of $O_2(a^1\Delta_g, v=0)$ concentration. In Table 4 the quantum yields of $O_2(X^3\Sigma_g^-, v=0–5)$ in the reaction of collisions of $O_2(a^1\Delta_g, v=0)$ with O_2 (Wild et al., 1984) are presented.

The values of the rate constants of the reactions of deexcitation of electronically-vibrationally excited O_2 molecules $O_2(a^1\Delta_g, v\geq1)$ at collisions with N_2 are so small that such processes do not affect the populations of electronic-vibrational levels under consideration in comparison with the processes of deexcitation at collisions with molecular oxygen. For estimations we used the maximum value for these rate constants $8.4\times10^{-14}\,cm^3\,s^{-1}$ from Klais et al. (1980), which is two orders of magnitude smaller than the rate constants of the processes of deexcitation at collisions with molecular oxygen.

The role of quenching electronically excited molecules $O_2(a^1\Delta_g, v=0)$ by N_2 is significant, and the corresponding process was taken into account (see Table 4).

In Table 5 the rate constants of V-V and V-T processes of $O_2(X^3\Sigma_g^-, v)$ collisional excitation and deexcitation are presented. In order to calculate the populations of vibrational levels for v=1–35, approximations of the dependencies of rate constants on vibrational quantum numbers on the basis of the known experimental data must be carried out. The presented approximations (see Table 5) give a convenient form for the calculations of the values of the rate constants used in our model within the limits of experimental data errors. With the purpose of constructing kinetic equations for $v\leq35$, the rate constants of V-T deexcitation of $O_2(X^3\Sigma_g^-, v)$ in collisions with O_2 calculated for $v\leq30$ (Coletti and Billing, 2002) were extrapolated for $v\leq35$.

The ozone and oxygen photodissociation is a non-equilibrium stationary process. For a description of such kind of processes, using the principle of detailed equilibrium is inapplicable for the calculation of the rate constant of the inverse process of the upper state excitation by the transition from the lower state. This is why we don't use the principle of detailed equilibrium for calculations of populations of the considered electronic-vibrational states. For inverse processes of V-V and V-T energy transfer between vibrational states of the ground electronic state $O_2(X^3\Sigma_g^-, v)$, we use the rate constants calculated by Billing et al. (1992); Coletti and Billing (2002) from the measured cross sections of collisional reactions. The inverse processes of populating the electronically-vibrationally excited states $O_2(b^1\Sigma_g^+, v)$ and $O_2(a^1\Delta_g, v)$ are insignificant in comparison with the processes of populating from the upper states or directly by photodissociation, because the energy difference is greater than 1 eV. The estimations show that in our model we can neglect these processes.

The experimental methods of the measurements of the rate constants of deexcitation processes could be conventionally divided into two groups: measurements for low (200–400 K) and those for high temperatures, for example, experiments in shock tubes, which were carried out at the temperatures of higher than one thousand Kelvins. It should be noted that at high temperatures the measured rate constant might be a superposition of the rate constants for several states (Polack, 1979). In accordance with the atmospheric conditions, we use the values of the rate constants measured in the temperature interval 150–350 K.

At conditions when the local thermodynamic equilibrium (LTE) for electronic-vibrational states does not exist, the populations of the states are calculated by solving the system of kinetic equations for all 45 electronic-vibrational states under consideration: the first excited state of atomic oxygen, $O(^1D)$, three states of $O_2(b^1\Sigma_g^+, v)$, six states of $O_2(a^1\Delta_g, v)$ and 35 states of $O_2(X^3\Sigma_g^-, v)$.

The populations of the states of these excited species are described by the system of differential equations:

$$\frac{\partial n_i}{\partial t} = \sum_{k\neq i}(n_k \cdot p_{i,k}) - n_i \cdot q_i + F_i, \tag{19}$$

where i – the state number (i=1–45), n_i – the population of the i-th state, $p_{i,k}$ – the production rate of species i from species k (k=1–45, $k\neq i$) in collisional processes of energy transfer, q_i – the total loss rate of species i in the processes of collisional and radiative deactivation, F_i – the volume production rate of the i-th species in the processes of photolysis of O_2 and O_3 molecules and in chemical reactions (for example, in the reaction of collision of O with O_3).

Then the system of differential Eqs. (19) can be presented as a matrix equation for the vector of the state populations $\boldsymbol{n}$

$$\frac{\partial \boldsymbol{n}}{\partial t} = \mathbf{A}\cdot\boldsymbol{n} + \boldsymbol{F}. \tag{20}$$

We are solving a stationary problem. In this case the system of equations is written as a linear algebraic system

$$\boldsymbol{n} = \mathbf{A}^{-1}\cdot\boldsymbol{F}. \tag{21}$$

The matrix $\mathbf{A}$ is a quasi-diagonal square sparse matrix. The method of solving the system of equations is described in

Olemskoy (2006). In order to derive the ozone concentration from the measured intensities of emissions, the system of implicit algebraic equations is solved by the method of parameter fitting.

The computer code for calculating the rate of photodissociation of ozone and molecular oxygen, taking into account the spectral dependence of quantum yields of the products of O_2 and O_3 photolysis in the interval of wavelengths from 120 to 850 nm, was developed. The computer code enables us to calculate the rates of: 1) the formation of $O(^1D)$ atoms in the O_2 photolysis in the Schumann-Runge continuum and in the Lyman-α line (3) and O_3 photolysis in the Hartley band (4); 2) the formation of $O_2(a^1\Delta_g, v)$ in O_3 photolysis in the Hartley band (4); 3) the formation of $O_2(X^3\Sigma_g^-, v)$ in O_3 photolysis in the Hartley, Chappius and Huggins bands (12) for different solar zenith angles (from $-80°$ to $80°$ SZA). In our calculations of the photodissociation rate, the model of photodissociation in the Schumann-Runge continuum, suggested by DeMajistre et al. (2001), and the model of photodissociation in the Schumann-Runge bands, suggested by Koppers and Murtagh (1996), were used. In the code model MSIS 90 was used for the main atmospheric constituents, the O_3 model was taken from Keating et al. (1989), the atomic oxygen model was taken from Llewellyn and McDade (1996), the CO_2 model was taken from Kauffmann et al. (2002). The solar spectrum was taken from Allen and Frederick (1982). The photodissociation cross sections of the solar radiation for the Hartley bands were taken from DeMore et al. (1997).

In this way, the developed method enables us to calculate the altitude profiles of the concentration of O_2 molecules in any considered electronic-vibrational state in the middle atmosphere. However, at present, only the information about the populations of $O_2(a^1\Delta_g, v=0)$ and $O_2(b^1\Sigma_g^+, v=0)$ can be obtained from the atmospheric experiments. In principle, the formulation and solution of the inverse problem for any state under consideration is possible, but the accuracy of the solution for upper states decreases because the values of the rate constants are less known and the populations of these states are much smaller than for the lower states.

3 Concentrations of electronically-vibrationally excited oxygen in the middle atmosphere

The proposed model was used to calculate the altitude profiles of the number densities of O_2 molecules in electronic-vibrational states. The calculations were made for the conditions of the experiment METEORS (Mlynczak et al., 2001), in which both emissions at 762 nm and 1.27 μm were measured simultaneously. It was carried out for 32° N and for the Solar zenith angle 38°.

In Fig. 2 the altitude profiles of the number densities of the molecules in the states $O_2(b^1\Sigma_g^+, v)$ for v=0, 1 and 2 and the measured number densities of $O_2(b^1\Sigma_g^+, v=0)$ (Mlynczak et al., 2001) are shown. With the purpose of showing how the choice of the $[O_3]$ profile other than the one from Keating et al. (1989) changes the results, the altitude profiles of the number densities of molecules in the states $O_2(b^1\Sigma_g^+, v)$ for v=0 and 1 were also calculated for two other ozone altitude profiles $[O_3]'$, for variations of $[O_3]'/[O_3]$ equal to 0.5 and 2.0.

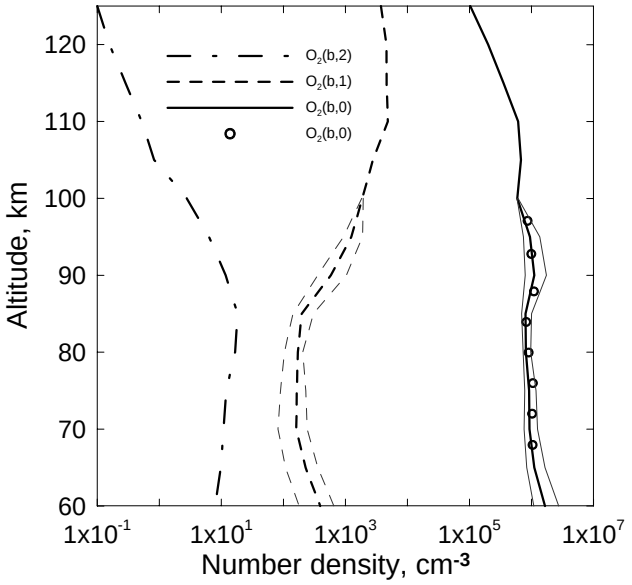

Fig. 2. Altitude profiles of the number densities of the molecules in the state $O_2(b^1\Sigma_g^+, v)$ for v=0, 1 and 2. Circles – experimental data of METEORS for $O_2(b^1\Sigma_g^+, v=0)$ (Mlynczak et al., 2001). The bold curves – calculations for the conditions of experiment METEORS in accordance with our model. The altitude profiles of the number densities of molecules in the states $O_2(b^1\Sigma_g^+, v)$ for v=0 and 1, calculated for two ozone altitude profiles $[O_3]'$ at variations of $[O_3]'/[O_3]$ equal to 0.5 and 2.0, are shown by thin grey lines.

In Fig. 3 the relative contributions of different processes to the total rate of production of $O_2(b^1\Sigma_g^+, v=0)$ are shown. In correspondence with the fact that above 85 km the main process of the $O_2(b^1\Sigma_g^+, v=0, 1)$ population is the Reaction (5) (channels 3 and 4 in Fig. 3), the ratio between the populations of vibrational levels v=0 and 1 correlates with the quantum yields of the $O_2(b^1\Sigma_g^+, v=0)$ and $O_2(b^1\Sigma_g^+, v=1)$ formation in this reaction (see Fig. 2). At 125 km, where the process of radiative deactivation dominates among the processes of deexcitation, the results of our calculations show that the ratio $[O_2(b^1\Sigma_g^+, v=1)]/[O_2(b^1\Sigma_g^+, v=0]$ becomes the same as the ratio of the quantum yields: 0.40/0.55. Below 100 km the contribution of the processes of the $O_2(b^1\Sigma_g^+, v=0, 1)$ population due to the absorption of solar radiation at 762 nm and 689 nm becomes important (channels 5 and 2 in the Fig. 3). The drastic reduction in the $O_2(b^1\Sigma_g^+, v=1)$ concentration in comparison with the concentration of the $O_2(b^1\Sigma_g^+, v=0)$ at the altitudes below 90 km (see Fig. 2) is governed by the fast reaction of the EE exchange $O_2(b^1\Sigma_g^+, v=1)+O_2(X^3\Sigma_g^-,$

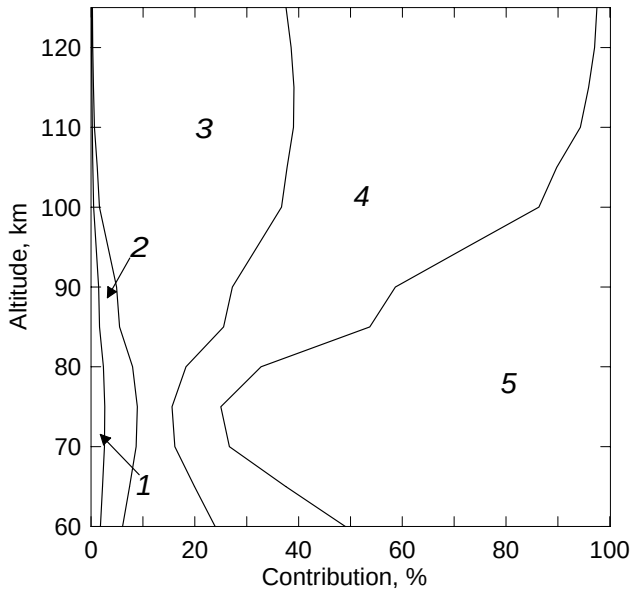

Fig. 3. Areas of diagram indicate the relative contributions of direct and indirect processes to the total rate of $O_2(b^1\Sigma_g^+, v=0)$ production, in percent. Indirect processes: 1 – absorption of solar radiation $O_2+h\nu$ (629 nm)$\rightarrow O_2(b^1\Sigma_g^+, v=2)$ (magnified by 10); 2 – absorption of solar radiation $O_2+h\nu$ (689 nm)$\rightarrow O_2(b^1\Sigma_g^+, v=1)$; 3 – energy transfer $O(^1D)\rightarrow O_2(b^1\Sigma_g^+, v=1)$. Direct processes: 4 – energy transfer $O(^1D)\rightarrow O_2(b^1\Sigma_g^+, v=0)$; 5 – absorption of solar radiation $O_2+h\nu$ (762 nm)$\rightarrow O_2(b^1\Sigma_g^+, v=0)$.

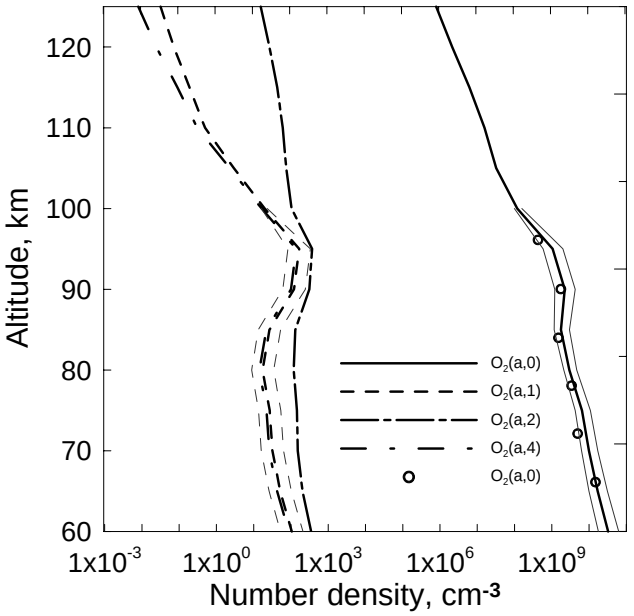

Fig. 4. Altitude profiles of the number densities of the molecules in the states $O_2(a^1\Delta_g, v)$ for v=0, 1, 2 and 4. The bold curves – calculations for the conditions of experiment METEORS (Mlynczak et al., 2001) in accordance with our model. Circles – experimental data of METEORS for $O_2(a^1\Delta_g$. v=0) (Mlynczak et al., 2001). The altitude profiles of number densities of molecules in the states $O_2(a^1\Delta_g, v)$ for v=0 and 1, calculated for two ozone altitude profiles $[O_3]'$ at variations of $[O_3]'/[O_3]$ equal to 0.5 and 2.0, are shown by thin grey lines.

v=0)$\rightarrow O_2(X^3\Sigma_g^-, v=1)+O_2(b^1\Sigma_g^+, v=0)$. The minimum of the contributions of channels 3 and 4 in Fig. 3 at 70–80 km is connected to the fact that below 80 km the channel of the $O(^1D)$ formation in the O_2 photolysis in the Schumann-Runge continuum (Eq. 3), dominating at higher altitudes, gives way to the formation of $O(^1D)$ in ozone photolysis in the Hartley band (4).

In Fig. 4 the altitude profiles of the number densities of the molecules in the states $O_2(a^1\Delta_g, v)$ for v=0, 1, 2 and 4 and the measured number densities of $O_2(a^1\Delta_g, v=0)$ (Mlynczak et al., 2001) are shown, although the calculations were also made for v=3 and 5. With the purpose of showing how the choice of the $[O_3]$ profile other than the one from Keating et al. (1989) changes the results, the altitude profiles of the number densities of the molecules in the states $O_2(a^1\Delta_g, v)$ for v=0 and 1 were also calculated for two variations of $[O_3]'/[O_3]$, equal to 0.5 and 2.0.

In Fig. 5 the relative contributions of the different processes to the total rate of production of O_2 ($a^1\Delta_g$, v=0) are shown. The $O_2(a^1\Delta_g, v=0)$ population is governed by ozone photolysis in the Hartley band (channels 2 and 3 in Fig. 5) and the energy transfer in the processes $O(^1D)\rightarrow O_2(b^1\Sigma_g^+, v)\rightarrow O_2$ ($a^1\Delta_g$, v) (channel 4 in Fig. 5). The local maximum of contributions of the channels 2 and 3 at the region of 90 km in Fig. 5 is connected with the local ozone maximum at this altitude. The ratio between the direct and indirect processes of the O_2 ($a^1\Delta_g$, v=0) population strongly depends on altitude (see Fig. 5). The indirect process occurs by means of fast reactions: first, an EE energy exchange O_2 ($a^1\Delta_g$, v>1)+$O_2(X^3\Sigma_g^-, v=0)\rightarrow O_2(X^3\Sigma_g^-, v)+O_2$ ($a^1\Delta_g$, v=0); second, VT-quenching at collisions with atomic oxygen O_2 ($a^1\Delta_g$, v)+$O(^3P)\rightarrow O_2$ ($a^1\Delta_g$, v=0)+$O(^3P)$ (see Table 4).

Figure 4 shows that the vertical profiles of the O_2 ($a^1\Delta_g$, v≥1) concentrations significantly differ by shape from the [O_2 ($a^1\Delta_g$, v=0)] profile. The concentrations of O_2 ($a^1\Delta_g$, v≥1) are much smaller than the O_2 ($a^1\Delta_g$, v=0) concentration, because the O_2 ($a^1\Delta_g$, v≥1) states are rapidly deactivated in the process of the EE energy exchange (see Table 4). The radiative deexcitation is not significant for the entire altitude interval. Thus, as EE energy exchange is a much faster process than the processes of V-V exchange between the vibrational sublevels of the electronic state O_2 ($a^1\Delta_g$), the relative populations of O_2 ($a^1\Delta_g$, v≥1), except for O_2 ($a^1\Delta_g$, v=2), reflect the initial populations of the vibrational sublevels O_2 ($a^1\Delta_g$, v) formed in O_3 photolysis (see Table 1). This is why the concentrations of O_2 ($a^1\Delta_g$, v≥1) below 100 km are close to each other and the vertical profiles of the O_2 ($a^1\Delta_g$, v≥1) concentrations, with the exception of

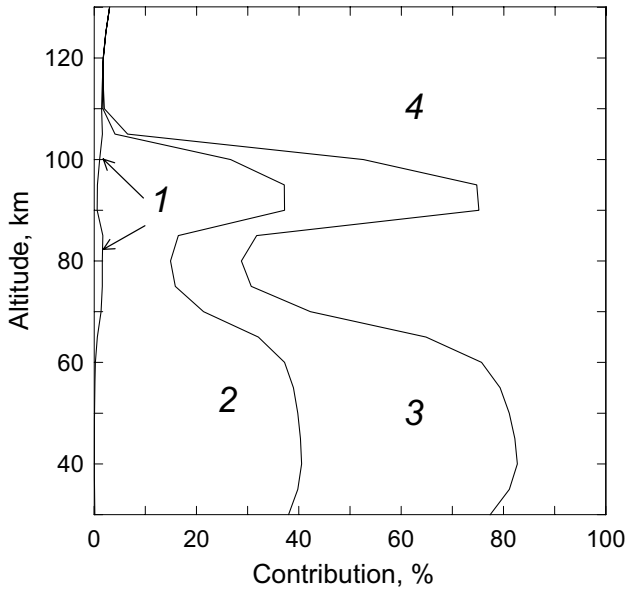

Fig. 5. Areas of diagram indicate the relative contributions of direct and indirect processes to the total rate of $O_2(a^1\Delta_g, v=0)$ production, in percent. Direct processes: 1 – absorption of solar radiation $O_2+h\nu$ (1.27 μm)$\rightarrow O_2(a^1\Delta_g, v=0)$; 2 – ozone photolysis in the Hartley band $O_3+h\nu\rightarrow O_2(a^1\Delta_g, v=0)$. Indirect processes: 3 – ozone photolysis in the Hartley band $O_3+h\nu\rightarrow O_2(a^1\Delta_g, v\geq 1)$; 4 – energy transfer $O(^1D)\rightarrow O_2(b^1\Sigma_g^+, v)\rightarrow O_2(a^1\Delta_g, v)$.

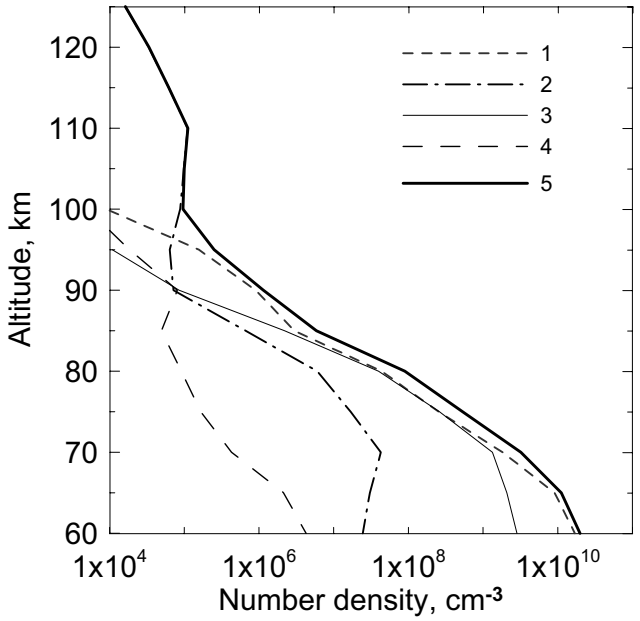

Fig. 6. Altitude profile of the number densities of the molecules in the state $O_2(X^3\Sigma_g^-, v=1)$ calculated selectively for four main non-LTE channels if only one channel has been taken into account for the conditions of experiment METEORS (Mlynczak et al., 2001) in accordance with our model: 1 – ozone photolysis in the Hartley, Huggins and Chappius bands; 2 – photolysis of O_2 in the Shumann-Runge continuum and Lyman-α; 3 – absorption by O_2 of solar radiation at 689 and 762 nm bands; 4 – reaction $O_3+O\rightarrow O_2(X^3\Sigma_g^-, v)+O_2$ (see Table 5); 5 – total density (all channels are taken into account).

$[O_2\ (a^1\Delta_g, v=2)]$, are similar by shape and correlate with the profile of the ozone concentration. As can be seen from Fig. 4, the $[O_2\ (a^1\Delta_g, v=2)]$ are higher than the $[O_2\ (a^1\Delta_g, v=1, 4)]$ for the entire altitude interval, because $O_2\ (a^1\Delta_g, v=2)$ is populated additionally by the quasi-resonance process of quenching of $O_2(b^1\Sigma_g^+, v=0)$ at collisions with N_2 (see the discussion of Table 3 in Sect. 2).

The model also enables us to calculate the number densities of O_2 in the ground electronic state with the vibrational quantum number from 1 to 35. As can be seen from Fig. 1 and Table 5, high vibrational levels of the $O_2(X^3\Sigma_g^-)$ and also energy transfer from $O_2(b^1\Sigma_g^+, v)$ and $O_2\ (a^1\Delta_g, v)$ should be considered for correct calculations of the concentration of the $O_2(X^3\Sigma_g^-, v=1)$.

In Fig. 6 the altitude profile of the $O_2(X^3\Sigma_g^-, v=1)$ concentration and the contributions of different channels of the $O_2(X^3\Sigma_g^-, v=1)$ population are shown. As can be seen from Fig. 6, ozone photolysis in the Hartley, Huggins and Chappius bands is the main channel of the $O_2(X^3\Sigma_g^-, v=1)$ population up to 95 km, however, in the range 70–85 km the absorption of solar radiation by oxygen at 689 and 762 nm gives almost the same contribution. Above 95 km ozone photolysis gives way to oxygen photolysis in the Shumann-Runge continuum and in the Lyman-α. As can be concluded from our calculations, vibrational excitation of O_2 in the reaction of ozone with atomic oxygen (Table 5) is insignificant during daytime (curve 4 in Fig. 6).

The altitude profiles of the concentration of $O_2(X^3\Sigma_g^-, v=1)$ were calculated with the purpose of solving the problem of non-equilibrium radiation of H_2O in the 6.3-μm band in the middle atmosphere. The process of quasi-resonance V-V energy exchange between the first excited vibrational levels of the H_2O and O_2 molecules is very fast; this is why it is important to take into account this source of vibrational excitation of $H_2O(010)$ (Manuilova et al., 2001).

4 762-nm and 1.27-μm emissions in the middle atmosphere

We used our new model to calculate the concentrations of $O_2(a^1\Delta_g, v=0)$ and $O_2(b^1\Sigma_g^+, v=0)$ and, correspondingly, the intensities of the 1.27-μm and 762-nm emissions in the middle atmosphere.

It should be stressed that the model of pure electronic kinetics is a particular case of the model of electronic-vibrational kinetics. The electronic kinetics model can be obtained from the electronic-vibrational kinetics model by the following assumptions: 1) – only electronically excited products are formed in O_3 photolysis; 2) – the processes of energy

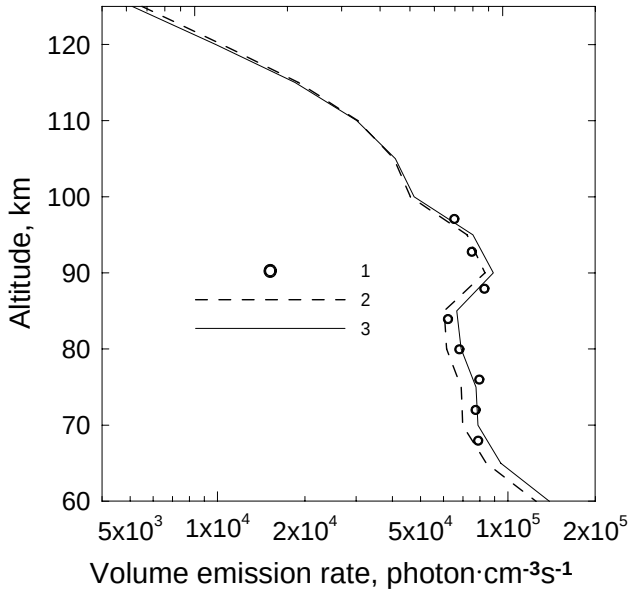

Fig. 7. Volume emission rate at 762 nm. Circles (1) – experimental data of METEORS (Mlynczak et al., 2001). Curves – calculations for the conditions of experiment METEORS: 2 – in accordance with the model of Mlynczak et al. (1993); 3 – in accordance with our model.

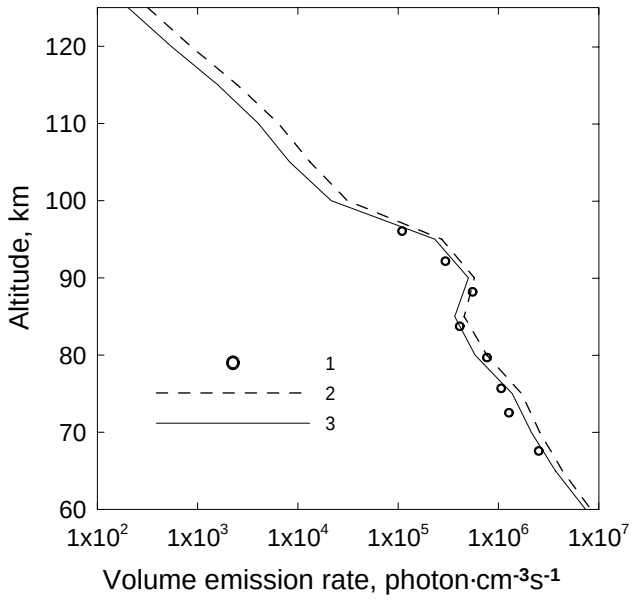

Fig. 8. Volume emission rate at 1.27 μm. Circles (1) – experimental data of METEORS (Mlynczak et al., 2001). Curves – calculations for the conditions of experiment METEORS: 2 – in accordance with the model of Mlynczak et al. (1993); 3 – in accordance with our model.

transfer between electronic states at collisions occur without vibrational excitation. Accordingly, only 17 processes remain from more than 100 listed in Tables 1–5. This model totally corresponds to the model of Mlynczak et al. (1993). All calculations presented below have been made for both models; the pure electronic model is called by us as the model of Mlynczak et al. (1993).

Figure 7 presents the comparison of the experimental data on the vertical profile of the volume emission rate at the wavelength of 762 nm (Mlynczak et al., 2001) and the calculations for the experimental conditions provided by our model and the model of only electronic kinetics.

In the same experiment (Mlynczak et al., 2001), the intensity of the 1.27-μm emission was measured simultaneously with the 762-nm emission. In Fig. 8 the experimental data on the vertical profile of the volume emission rate at the wavelength of 1.27-μm are compared with the calculations for the experimental conditions provided by our model and the model of Mlynczak et al. (1993). For the entire altitude interval, the values of the volume emission rate at the wavelength of 1.27 μm, calculated in accordance with our model, are lower than the results calculated in accordance with the model of Mlynczak et al. (1993). The discrepancy between the volume emission rates at 1.27 μm, calculated in accordance with the electronic-vibrational kinetics model, and the pure electronic model is 15–60% at the region of 60–125 km.

5 Retrieval of the vertical ozone profile from the measured intensity profiles of the 762-nm and 1.27-μm emissions

We will show that consideration of electronic-vibrational kinetics is very important for the problem of ozone retrieval from the measurements of the intensity in the Atmospheric and IR Atmospheric bands of the O_2 molecule. For the purpose of revealing which errors evolve due to the use of the pure electronic kinetics, we carried out the following numerical experiments.

For the first numerical experiment, the test ozone mixing ratio vertical profiles were taken from Marsh et al. (2002), where HRDI instrument observations of ozone in the mesosphere and lower thermosphere are presented. The "measured" volume emission rates in the 762-nm and 1.27-μm bands were calculated for the test ozone mixing ratio in accordance with the electronic-vibrational kinetics model for the atmospheric conditions of this experiment. In the second stage, the inverse problem of ozone vertical profile retrieval from the "measured" volume emission rates in the 762-nm and 1.27-μm bands was solved in accordance with the pure electronic model of Mlynczak (1993). Figure 9 shows that there is a considerable discrepancy between the retrieved ozone vertical profiles and the test ones (for March and December HRDI data) in the whole altitude range of 65–97 km. The maximum discrepancy between the retrieved ozone mixing ratio and the test one occurs at about 75 km. For March, this discrepancy reaches 25% for the ozone

mixing ratio retrieved from the 762-nm emission, and for the 1.27-μm emission the retrieved ozone mixing ratio is two times smaller than the test one. For December, at 75 km the discrepancy reaches 14% for the ozone mixing ratio retrieved from 762-nm emission and 33% for the ozone mixing ratio retrieved from 1.27-μm emission. From the numerical experiment which was described above, it can be concluded, that in the framework of pure electronic kinetics the retrieval of the ozone mixing ratio from the 762-nm emission is preferable to the retrieval from the 1.27-μm emission.

The second numerical experiment is the interpretation of the atmospheric experiment on the retrieval of the vertical ozone profile from simultaneous measurements of the intensity in the Atmospheric and IR Atmospheric bands of the O_2 molecule carried out in the experiment METEORS (Mlynczak et al., 2001). Using our model and the model of Mlynczak et al. (1993), we have solved the inverse problem of the [O_3] determination from the METEORS volume emission rates at 762 nm and 1.27 μm presented in Mlynczak et al. (2001). Figure 10 presents the results of the retrieval of the ozone concentration.

Above 65 km, according to our model, the vibrational-electronic kinetics of the products of O_3 and O_2 photolysis play an important role in the mechanism of the formation of these emissions. As a result, above 65 km the retrievals of [O_3] by our model and the model of Mlynczak et al. (1993) differ significantly.

In accordance with the calculations for the model of Mlynczak et al. (1993), in the region near 85–90 km, the O_3 concentration retrieved from the intensity of the O_2 band at 762 nm is 45–30% greater than the O_3 concentration retrieved from the intensity of the O_2 band at 1.27 μm (see dashed lines in Fig. 10).

For our model the vertical [O_3] profiles retrieved from both emissions are closer to each other, and in the altitude range of 80–90 km the discrepancy is 20–17% (solid lines in Fig. 10). The [O_3] value retrieved from the intensity of the 1.27-μm band, in accordance with our model in the range of the local ozone peak at 80–90 km, is 40–15% as large as that obtained for the model of Mlynczak et al. (1993) (lines 3 and 4 in Fig. 10).

As can be seen from both numerical experiments (Figs. 9, 10), up to 90 km the differences between the ozone abundances retrieved in accordance with our model and the model of pure electronic kinetics of O_3 and O_2 photolysis from the emission at 762 nm are much smaller than the corresponding difference between the ozone abundances retrieved in accordance with both models from the 1.27-μm emission. Mlynczak et al. (1993) considered only populating $O_2(b^1\Sigma_g^+$, v=0), using the total rate constant of collisions of $O(^1D)$ with O_2. We considered the process of populating the electronic-vibrational levels $O_2(b^1\Sigma_g^+$, v=0, 1), using the same total rate constant, but taking into account the quantum yields of the $O_2(b^1\Sigma_g^+$, v=0) and the $O_2(b^1\Sigma_g^+$, v=1) formation in this reaction. However, the state $O_2(b^1\Sigma_g^+$, v=1) is deactivated by the mechanism of EE deexcitation to the level v=0 (Table 3). This is why the ozone concentrations retrieved from the 762-nm emission, in accordance with our model, and with the pure electronic model are closer to each other than those retrieved from the 1.27-μm emission.

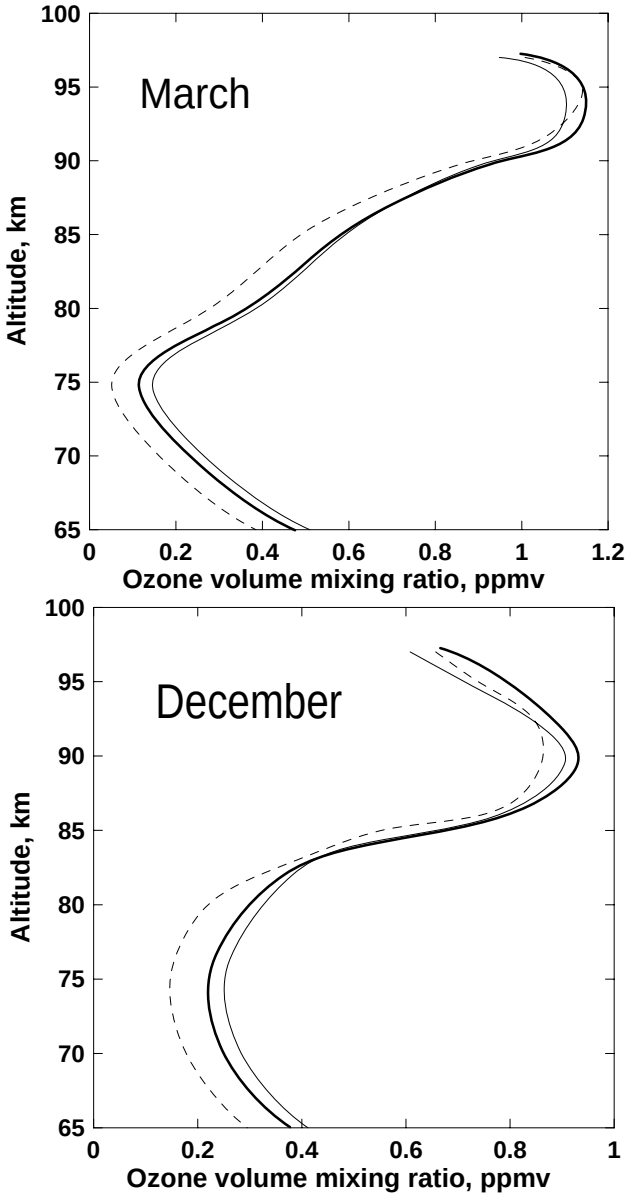

Fig. 9. Altitude profiles of ozone concentration retrieved from "measured" O_2 emissions at 762 nm (thin solid line) and 1.27 μm (dashed line) in accordance with pure electronic kinetics model. "Measured" volume emission rates at 762 nm and 1.27 μm were calculated in accordance with electronic-vibrational kinetics model at using HRDI ozone profiles for March and December (thick solid line) (Marsh et al., 2002).

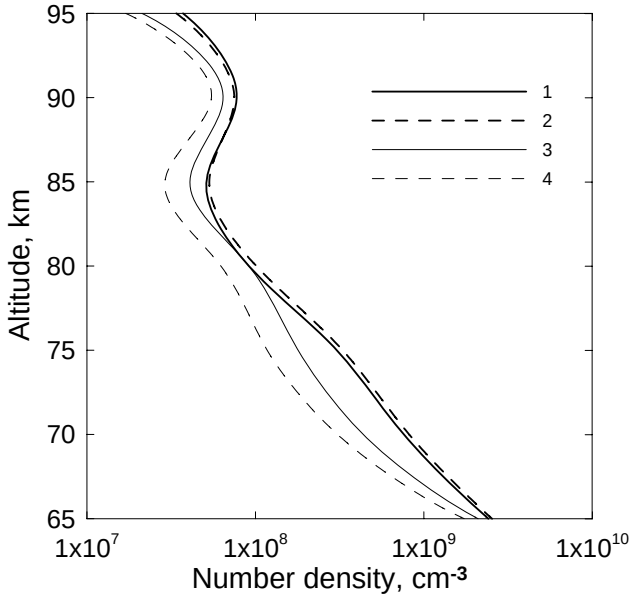

Fig. 10. Altitude profiles of ozone concentration retrieved from simultaneous observations of O_2 emissions at 762 nm and 1.27 μm in METEORS (Mlynczak et al., 2001). Retrievals in accordance with: our model – solid lines, model of Mlynczak et al. (1993) – dashed lines. Curves 1 and 2 – retrievals from measurement of emission at 762 nm $O_2(b^1\Sigma_g^+, v=0 \rightarrow X^3\Sigma_g^-, v=0)$. Curves 3 and 4 – retrievals from measurement of emission at 1.27 μm $O_2(a^1\Delta_g, v=0 \rightarrow X^3\Sigma_g^-, v=0)$.

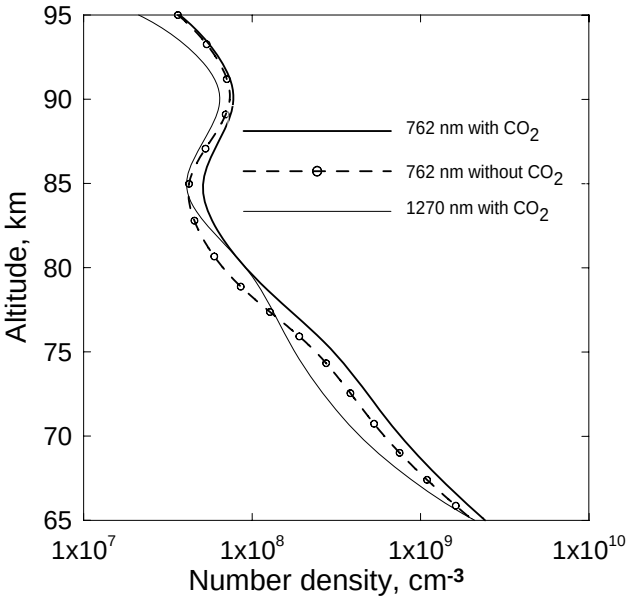

Fig. 11. Altitude profiles of ozone concentration retrieved from simultaneous observations of O_2 emissions at 762 nm and 1.27 μm in METEORS (Mlynczak et al., 2001). Retrievals in accordance with our model: taking into account CO_2 altitude profile – solid lines, with CO_2 mixing ratio equal to 0 – dashed lines.

Based on the results of ozone retrievals from emissions at 762 nm and 1.27 μm, presented in Figs. 9 and 10, one can conclude that ozone abundance retrieval carried out in accordance with the model of only electronic kinetics of O_3 and O_2 photolysis (Mlynczak et al., 1993) from the emission at 762 nm, which is formed by the transition from the state $O_2(b^1\Sigma_g^+)$, is preferable to retrieving the profiles of ozone abundance from the Infrared Atmospheric band of O_2 emission at 1.27 μm, which is formed by the transition from the state $O_2(a^1\Delta_g)$. This conclusion is the opposite to the traditional point of view but is not surprising, because in our model it was shown that the mechanism of populating the $O_2(a^1\Delta_g, v)$ states is much more complicated than that of populating the $O_2(b^1\Sigma_g^+, v)$ states (see Fig. 1 and Tables 1–4).

It should be noted that we came to this assertion on the basis of the analysis of only two numerical experiments. The final conclusion about the errors introduced in the retrieved values of ozone concentrations when using the model of only electronic kinetics of O_3 and O_2 photolysis for retrieval of the profiles of ozone concentration from the measurements in the bands at 762 nm and 1.27 μm can only be made after analyzing a great deal of data (e.g. in the satellite experiment ODIN-OSIRIS both emissions are measured simultaneously during a long period of time; Murtagh et al., 2002).

It is interesting to point to the influence of CO_2 abundance on the retrieval of ozone concentrations from the measurements in the band at 762 nm which is connected with the high value of the rate constant of reaction of deexcitation of $O_2(b^1\Sigma_g^+, v=0)$ by CO_2, whereas the CO_2 concentration does not influence the retrieval of ozone concentration from the measurements in the band at 1.27 μm (Fig. 11). For the calculations presented in Fig. 11 we used the CO_2 altitude profile from Kauffmann et al. (2002), which gives a significant decrease in the CO_2 volume mixing ratio above 75 km.

Comparison of the ozone concentrations retrieved from the measurements in the band at 762 nm, taking into account the $[CO_2]$ altitude profile and with CO_2 mixing ratio equal to 0 in the whole altitude region shows, in the framework of our model, a sensitivity of ozone concentrations retrieval to the $[CO_2]$ altitude profile below 90 km (Fig. 11).

6 Conclusions

1. We have developed the model of kinetics of the excited products of ozone and oxygen photolysis, taking into account the processes of energy transfer between electronically-vibrationally excited states of the oxygen molecule of $O_2(a^1\Delta_g, v)$ and $O_2(b^1\Sigma_g^+, v)$, excited oxygen atoms $O(^1D)$, and oxygen molecules in the ground state $O_2(X^3\Sigma_g^-, v)$.

2. Above 65 km the previous model of electronic kinetics of the excited products of the ozone and oxygen photolysis should be replaced by the model of electronic-vibrational kinetics.

3. The proposed model allows for calculation not only of vertical profiles of the $O_2(a^1\Delta_g$, v=0) and $O_2(b^1\Sigma_g^+$, v=0) concentrations, but also of the profiles of $[O_2(a^1\Delta_g$, v≤5)] and $[O_2(b^1\Sigma_g^+$, v=0, 1, 2)]. Correspondingly, in accordance with our model, not only the intensity of the 1.27-μm and 762-nm emissions, but also the intensity of emissions formed by transitions from electronically-vibrationally excited levels, such as $O_2(b^1\Sigma_g^+$, v=1)→$O_2(X^3\Sigma_g^-$, v=0) at 689 nm and $O_2(b^1\Sigma_g^+$, v=2)→$O_2(X^3\Sigma_g^-$, v=0) at 629 nm, can be calculated in the middle atmosphere. The model also enables us to calculate the number densities of O_2 molecules in the ground electronic state with the vibrational quantum numbers from 1 to 35.

4. With the consideration of the electronic-vibrational kinetics of the excited products of the ozone and oxygen photolysis, the discrepancy between the altitude profiles retrieved from the simultaneously measured intensities of the 762-nm and 1.27-μm emissions in the experiment METEORS (Mlynczak et al., 2001) becomes significantly smaller than it was for only the electronic kinetics model. The developed model, in principle, gives an opportunity to retrieve the ozone density profiles from different emissions formed by transitions from electronically-vibrationally excited levels of singlet O_2 molecules in the middle atmosphere.

5. Based on the results of the numerical experiments on ozone retrievals (using the experimental ozone mixing ratio profiles from HRDI experiment (Marsh et al., 2002) and simultaneously measured emissions at 762 nm and 1.27 μm in the experiment METEORS (Mlynczak et al., 2001)), one can conclude that in the case of the pure electronic kinetics model the ozone abundance retrieval from the emission at 762 nm is preferable to retrieving the profiles of ozone abundance from the infrared Atmospheric band of O_2 emission at 1.27 μm. Using the 1.27-μm emission measurements for ozone concentration retrieval above 65 km is incorrect if the interpretation of experiments is carried out in accordance with models of pure electronic kinetics of O_3 and O_2 photolysis.

Acknowledgements. The authors thank T. G. Slanger (SRI International, California) and V. I. Fomichev (York University, Toronto) for providing urgently needed information and for fruitful discussions and also post-graduate student V. A. Kuleshova (St. Petersburg State University, St. Petersburg) and M. A. Shelyakhovskaya for technical assistance. This work was partly supported by RFBR grants N 02-05-65259 and 05-05-65318.

Topical Editor U.-P. Hoppe thanks N. N. Shefov and another referee for their help in evaluating this paper.

References

Allen, M. and Frederick, J. E.: Effective photodissociation cross sections for molecular oxygen and nitric oxide in the Schumann-Runge bands, J. Atmos. Sci., 39, 2066–2075, 1982.

Amimoto, S. T. and Wiensfeld, J. R.: $O_2(b^1\Sigma_g^+)$ production and deactivation following quenching of $O(^1D)$ in O_3/O_2 mixtures, J. Chem. Phys., 72, 3899–3903, 1980.

Atkinson, R., Baulch, D. L., Cox, R. A., Hampson Jr., R. F., Kerr, J. A. (Chairman), and Troe, J.: Evaluated kinetic and photochemical data for atmospheric chemistry supplement VI, IUPAC Subcommittee on Gas Kinetic Data Evaluation for Atmospheric Chemistry, J. Phys. Chem. Ref. Data, 26, 1329–1497, 1997.

Ball, S. M., Hancock, G., and Winterbottom, F.: Product channels in the near-UV photodissociation of ozone, Faraday Discuss., 100, 215–227, 1995.

Balakrishnan, N. and Billing, G. D.: Quantum-classical reaction path study of the reaction $O(^3P)+O_3(^1A_1)\rightarrow 2O_2(X^3\Sigma_g^-)$, J. Chem. Phys., 104, 23, 9482–9494, 1996.

Billing, G. D. and Kolesnick, R. E.: Vibrational relaxation of oxygen. State to state rate constants, Chem. Phys. Lett., 200, 382–386, 1992.

Braithwaite, M., Davidson, J. A., and Ogryzlo, E. A: $O_2(^1\Sigma_g^+)$ relaxation in collisions. I. The influence of long range forces in the quenching by diatomic molecules, J. Chem. Phys., 65, 771–778, 1976.

Breig, E. L.: Statistical model for the vibrational deactivation of molecular by atomic oxygen, J. Chem. Phys., 51(10), 4539–4547, 1969.

Bucholtz, A., Skinner, W. R., Abreu, V. J., and Hays, P. B.: The dayglow of the O_2 Atmospheric band system, Planet. Space Sci., 34, 1031–1035, 1986.

Coletti, C. and Billing, G. D.: Vibrational energy transfer in molecular oxygen collisions, Chem. Phys. Lett., 356, 14–22, 2002.

DeMajistre, R., Yee, J.-H., and Zhu, X.: Parameterizations of oxygen photolysis and energy deposition rates due to solar energy absorption in the Schumann-Runge continuum, Geophys. Res. Lett., 28(16), 3163–3166, 2001.

DeMore, W. B., Golden, D. M., Hampson, R. F., Howard, C. J., Kolb, C. E., and Molina, M. J.: Chemical kinetics and photochemical data for use in stratospheric modeling, JPL Publication, 97-4, 1–128, 1997.

Dylewski, S. M., Geiser, J. D., and Houston, P. L.: The energy distribution, angular distribution, and alignment of the $O(^1D)$ fragment from the photodissociation of ozone between 235 and 305 nm, J. Chem. Phys, 115, 7460–7473, 2001.

Green, J. G, Shi, J., and Barker, J. R.: Photochemical kinetics of vibrationally excited ozone produced in the 248 nm photolysis of O_2/O_3 mixtures, J. Phys. Chem. A, 104, 6218–6226, 2000.

Hady-Ziane, S., Held, B., Pignolet, P., Peyrous, R., and Coste, C.: Ozone generation in an oxygen-fed wire-to-cylinder ozonizer at atmospheric pressure, J. Phys. D: Appl. Phys., 25, 677–685, 1992.

Harris, R. D. and Adams, G. W.: Where does the $O(^1D)$ energy go?, J. Geophys. Res. A, 88, 4918–4928, 1983.

Hwang, E. S., Bergman, A., Copeland, R. A., and Slanger, T. G.: Temperature dependence of the collisional removal of $O_2(b^1\Sigma_g^+$, v=1 & 2) at 110–260 K, and atmospheric applications, J. Chem. Phys., 110, 18–24, 1999.

Kalogerakis, K. S., Copeland, R. A., and Slanger, T. G.: Collisional removal of $O_2(b^1\Sigma_g^+$, v=2, 3), J. Chem. Phys., 116, 4877–4885, 2002.

Kalogerakis, K. S., Copeland, R. A., and Slanger, T. G.: Vibrational energy transfer in $O_2(X^3\Sigma_g^-$, v=2, 3)+O_2 collisions at 330 K, J. Chem. Phys., 123, 044303, doi:10.1063/1.1982788, 2005.

Kaufmann, M., Gusev, O. A., Grossmann, K. U., Roble, R. G., Hagan, M. E., Hartsough, C., and Kutepov, A. A.: The vertical and horizontal distribution of CO_2 densities in the upper mesosphere and lower thermosphere as measured by CRISTA, J. Geophys. Res. D, 107, 8182, doi:10.1029/2001JD000704, 2002.

Keating, G. M., Pitts, M. C., and Chen, C.: Improved reference models for middle atmosphere ozone Book: Middle Atmosphere Program, Handbook for MAP, 31, 37–49, 1989.

Klais, O., Laufer, A. H., and Kurylo, M. J.: Atmospheric quenching of vibrationally excited $O_2(a^1\Delta_g)$, J. Chem. Phys., 73, 2696–2699, 1980.

Klingshirn, H. and Maier, M.: Quenching of the $O_2(a^1\Delta_g)$ state in liquid isotopes, J. Chem. Phys., 82, 714–719, 1985.

Koppers, G. A. A. and Murtagh, D. P.: Model studies of the influence of O_2 photodissociation parameterizations in the Schumann-Runge bands on ozone related photolysis in the upper atmosphere, Ann. Geophys., 14, 68–79, 1996, http://www.ann-geophys.net/14/68/1996/.

Krupenie, P. H.: The spectrum of Molecular Oxygen, J. Phys. Chem. Ref. Data, 1, 423–521, 1972.

Lee, L. C. and Slanger, T. G.: Observation on $O(^1D\rightarrow{}^3P)$ and $O_2(b^1\Sigma_g^+\rightarrow X^3\Sigma_g^-)$ following O_2 photodissociation, J. Chem. Phys., 69, 4053–4060, 1978.

Llewellyn, E. J. and McDade, I. C.: A reference model for atomic oxygen in the terrestrial atmosphere, Adv. Space Res., 18, 209–226, 1996.

Lopez-Gonzalez, M. J., Lopez-Moreno, J. J., and Rodrigo, R.: The altitude profile of the infrared atmospheric system of O_2 in twilight and early night: derivation of ozone abundance's, Planet. Space Sci., 40, 1391–1397, 1992.

Lopez-Puertas, M., Zaragoza, G., Kerridge, B. J., and Taylor, F. W.: Non-local thermodynamic equilibrium model for H_2O 6.3 and 2.7 μm bands in the middle atmosphere J. Geophys. Res. D, 100, 9131–9147, 1995.

Manuilova, R. O., Yankovsky, V. A., Semenov, A. O., Gusev, O. A., Kutepov, A. A., Sulakshina, O. N., and Borkov, Yu. G.: Non-equilibrium emission of the middle atmosphere in the IR ro-vibrational water vapor bands, Atmos. Oceanic Opt., 14, 864–867, 2001.

Marsh, D. R., Skinner, W. R., Marshall, A. R., Hays, P. B., Ortland, D. A., and Yee, J.-H.: High resolution Doppler imager observations of ozone in the mesosphere and lower thermosphere, J. Geophys. Res. D, 107(D19), 4390, doi:10.1029/2001JD001505, 2002.

Michelsen, H. A., Salawitch, R. J., Wennberg, P. O., and Anderson, J. G.: Production of $O(^1D)$ from photolysis of O_3, Geophys. Res. Lett., 21, 2227–2230, 1994.

Mlynczak, M. G., Solomon, S. C., and Zaras, D. S.: An updated model for $O_2(^1\Delta_g)$ concentrations in the mesosphere and lower mesosphere and implications for remote sensing of ozone at 1.27 μm, J. Geophys. Res. D, 98, 18 639–18 648, 1993.

Mlynczak, M. G. and Marshall, B. T.: A reexamination of the role of solar heating in the O_2 atmospheric and infrared Atmospheric bands, Geophys. Res. Lett., 23, 657–660, 1996.

Mlynczak, M. G., Morgan, F., Yee, J.-H., Espy, P., Murtagh, D., Marshall, B. T., and Schmidlin, F.: Simultaneous measurements of the $O_2(a^1\Delta_g)$ and $O_2(b^1\Sigma_g^+)$ airglows and ozone in the daytime mesosphere, Geophys. Res. Lett., 28, 999–1002, 2001.

Murtagh, D., Frisk, U., Merino, F., et al.: An overview of the Odin atmospheric mission, Can. J. Phys., 80, 309–319, 2002.

Olemskoy, I. V.: Updating of algorithm of allocation structural features, Vestn. S. – Petersburg Univ., Ser. 10: Prikl. Matem., 55–64, 2006.

Pejakovic, D. A., Wouters, E. R., Phillips, K. E., Slanger, T. G., Copeland, R. A., and Kalogerakis, K. S.: Collisional removal of by O_2 at thermospheric temperatures. J. Geophys. Res. A, 110, 03308, doi:10.1029/2004JA010860, 2005.

Polack, L. S.: Non equilibrium chemical kinetics. Science Press, Moscow, 1979.

Reddmann, T. and Uhl, R.: The H Lyman-α actinic flux in the middle atmosphere, Atmos. Chem. Phys., 3, 225–231, 2003, http://www.atmos-chem-phys.net/3/225/2003/.

Rodrigo, R., Lopez-Moreno, J. J., Lopez-Puertas, M., Moreno, F., and Molina, A.: Neutral atmospheric composition between 60 and 220 km: a theoretical model for mid-latitudes, Planet. Space Sci., 34, 723–743, 1986.

Sica, R. J. and Lowe, R. P.: Inferring middle atmospheric ozone height profiles from ground-based measurements of molecules oxygen emissions rates, 2. Comparison with the $O_2(a^1\Delta_g)$ (0, 1) band measurements at sunset, J. Geophys. Res. D, 98, 1051–1055, 1993a.

Sica, R. J. and Lowe, R. P.: Inferring middle atmospheric ozone height profiles from ground-based measurements of molecules oxygen emissions rates, 3. Can twilight measurements of the Atmospheric band be used to retrieve an ozone density profile, J. Geophys. Res. D, 98, 1057–1067, 1993b.

Skinner, W. R. and Hays, P. B.: Brightness of the O_2 Atmospheric bands in the daytime thermosphere, Planet. Space Sci., 33, 17–22, 1985.

Slanger, T. G.: Studies on highly vibrationally-excited O_2, AIAA-97-2502, 32nd Thermophysics Conference, 23–25 June 1997/Atlanta, GA1997, 1997.

Slanger, T. G. and Copeland, R. A.: Energetic oxygen in the upper atmosphere and the laboratory, Chem. Rev., 103, 4731–4765, 2003.

Sparks, R. K., Carlson, L. R., Snobatake, K., Kowalczyk, M. L., and Lee, Y.T.: Ozone photolysis: A determination of the electronic and vibrational state distributions of primary products, J. Chem. Phys., 72, 1401–1402, 1980.

Streit, G. E., Howard, C. J., Schmeltekopf, A. L., Davidson, J. A., and Schiff, H. I.: Temperature dependence of $O(^1D)$ rate constants for reactions with O_2, N_2, CO_2, O_3, H_2O, J. Chem. Phys., 65, 11, 4761–4764, 1976.

Svanberg, M., Pettersson, J. B. C., and Murtagh, D.: Ozone photodissociation in the Hartley band: A statistical description of the ground state decomposition channel $O_2(X^3\Sigma_g^-)$ + $O(^3P)$, J. Chem. Phys., 102, 8887–8896, 1995.

Thelen, M. A., Gejo, T., Harrison, J. A., and Huber, J. R.: Photodis-

sociation of ozone in the Hartley band: Fluctuation of the vibrational state distribution in the $O_2(a^1\Delta_g, v)$ fragment, J. Chem. Phys., 103, 7946–7955, 1995.

Thomas, R. J., Barth, C. A., Rusch, D. W., and Sanders, R. W.: Solar mesosphere explorer near-infrared spectrometer: Measurements of 1.27 μm radiances and the interference of mesospheric ozone, J. Geophys. Res., 89, 9569–9580, 1984.

Tully, J. C.: Collision complex model for spin forbidden reactions: Quenching of $O(^1D)$ by N_2, J. Chem. Phys., 61, 61–68, 1974.

Valentini, J. J., Gerrity, D. P., Phillips, D. L., Nieh, J.-C., and Tabor, K. D.: CARS spectroscopy of $O_2(a^1\Delta_g)$ from the Hartley band photodissociation of O_3: Dynamics of the dissociation , J. Chem. Phys., 86, 6745–6756, 1987.

Webster III, H. and Bair, E. J.: Ozone ultraviolet photolysis. IV. O_2*+$O(^3P)$ vibrational energy transfer, J. Chem. Phys., 56, 6104–6108, 1972.

Wild, E., Klingshirn, H., and Maier, M.: Relaxation of the $a^1\Delta_g$ state on pure liquid oxygen and in liquid mixtures of $^{(16)}O_2$ and $^{(18)}O_2$, J. Photochem., 25, 134–143, 1984.

Yankovsky, V. A.: Electronic-vibrational relaxation of $O_2(b^1\Sigma_g^+$, v=1,2) at collisions with ozone and molecular and atomic oxygen, (in Russian), Khim. Fiz., 10, 291–306, 1991.

Yankovsky, V. A. and Kuleshova, V. A.: Photodissociation of ozone in Hartley band. Analytical description of quantum yields of $O_2(a^1\Delta_g$, v=0-3) depending on wave length, (in Russian), Atmos. Oceanic Opt., 19, 576–580, 2006.

Yankovsky, V. A. and Manuilova, R. O.: New self-consistent model of daytime emissions of $O_2(^1\Delta_g)$ and $O_2(b^1\Sigma_g^+)$ in the middle atmosphere. Retrieval of vertical ozone profile from the measured intensity profiles of these emissions, Atmos. Oceanic Opt., 16, 536–540, 2003.

Yee, J. H., Guberman, S. L., and Dalgarno, A.: Collisional quenching of $O(^1D)$ by $O(^3P)$, Planet. Space Sci., 38, 647–652, 1990.